ELSEVIER

Polymer 43 (2002) 749–755

polymer

www.elsevier.com/locate/polymer

# Structural development and mechanical properties on immiscible and miscible blends from isotactic polypropylene and ethylene–1-hexene copolymers under uniaxial drawing

Elinor L. Bedia[a], Syozo Murakami[b,*], Kazunobu Senoo[b], Shinzo Kohjiya[b]

[a]*Materials Science Division, Industrial Technology Development Institute, Bicutan, Taguig, Metro-Manila, Philippines*
[b]*Laboratory of Polymer Condensed States, Institute for Chemical Research, Kyoto University, Uji, Kyoto-fu 611-0011, Japan*

Received 19 June 2001; received in revised form 11 September 2001; accepted 28 September 2001

**Abstract**

Isotactic polypropylene and ethylene–1-hexene copolymers containing 32 and 57 mol% of 1-hexene copolymers blends (*i*-PP/EH32 and *i*-PP/EH57) were prepared by solution blending, precipitating followed by drying and hot pressing. The two blends were subject to investigation on structure and mechanical properties of these blends under uniaxial drawing. The *i*-PP/EH32 and *i*-PP/EH57 represented the immiscible and miscible blends, respectively. The tensile stresses and strains at breaking point of *i*-PP/EH57 were remarkably higher than those of *i*-PP/EH32 at room temperature. From wide-angle X-ray diffraction (WAXD) measurement, it was observed that the orientation of crystallites occurred early and then propagated gradually up to about drawing ratio 8 because chains of EH57 copolymer were incorporated into the amorphous regions between lamellae of *i*-PP. In the WAXD patterns of *i*-PP/EH57, the oriented spot reflections coexsisted with unoriented ring reflections up to draw ratio higher than in pure *i*-PP. On the other hand, the two-phase structure was observed from TEM and AFM in *i*-PP/EH32, and on the drawing, separation at the interface between two-phase was observed in *i*-PP/EH32 even at the low strain.


*Keywords*: *i*-Polypropylene and ethylene–1-hexene copolymer blend; Uniaxial drawing; Orientation

## 1. Introduction

Isotactic polypropylene (*i*-PP) is often blended with an elastomer to improve its impact performance at low temperatures. In the previous studies, *i*-PP had been blended with various elastomers such as ethylene–propylene rubbers [1–5] (e.g. ethylene–propylene copolymer and ethylene–propylene diene copolymer), styrene-*b*-ethylene-*co*-butylene-*b*-styrene triblock copolymer [6–9] and polybutadiene [10]. However, most of these polymers are incompatible with *i*-PP and the increase in their impact strength varies; some increase significantly [1–9], others are low [10]. The mechanical properties, e.g. tensile strength of these blends decrease with the increase in elastomer content and this limits their applications.

Recently, Yamaguchi and his co-workers [11–15] developed rubbery ethylene–α-olefin copolymers, i.e. ethylene–1-butene and ethylene–1-hexene copolymers (EB and EH, respectively). When blended with *i*-PP, they have found that these copolymers are immiscible with *i*-PP in the molten state if the α-olefin content is less than 50 mol% and miscible with amorphous phase of *i*-PP if it is more than 50 mol%. During crystallization, the EH molecules of the immiscible blends were observed to be in globular domains dispersed in the *i*-PP matrix, while in the miscible blends, the EH molecules were incorporated in the interlamellar and/or interfibrillar regions of *i*-PP spherulites [14]. Furthermore, the spherulite growth rate of immiscible blends was identical with that of pure *i*-PP and decreased in the miscible blends [14]. The miscibility of EH and EB with the amorphous part of *i*-PP resulted in a significant improvement in their mechanical properties [11], e.g. they are possible to be drawn at low temperatures (−20°C).

In plastics processing, the resins usually undergo stretching or drawing either uniaxially or biaxially to improve their mechanical strength. Therefore, the study on structure formation during stretching would provide additional information of much value in the optimization of processing parameters. In this report, such study is undertaken by uniaxial drawing of the immiscible and miscible blends (*i*-PP/EH32 and *i*-PP/EH57) of isotactic polypropylene

* Corresponding author. Tel.: +81-774-38-3064; fax: +81-774-38-3067.
*E-mail address:* murasyo@scl.kyoto-u.ac.jp (S. Murakami).

0032-3861/02/$ - see front matter 
PII: S0032-3861(01)00653-X

and ethylene–1-hexene copolymers and the structural changes are measured using in situ wide-angle X-ray diffraction (WAXD) technique. The blends were also characterized using SAXS, AFM, TEM and tensile measurements.

## 2. Experimental

### 2.1. Polymers and blending

Isotactic polypropylene (*i*-PP) and ethylene–1-hexene copolymers containing 32 and 57 mol% of 1-hexene copolymers (EH32 and EH57) used in the study were kindly supplied by JGS Petrochemical Corp., Philippines and TOSOH Corp., Japan, respectively. EH32 and EH57 copolymers were synthesized with a metallocene catalyst. The *i*-PP was an injection molding grade thermoplastic resin with an average molecular weight of $2.7 \times 10^5$ and melt flow index of 8 g/10 min. EH32 and EH57 copolymers contained 1-hexene chains of 31.8 and 57.1 mol% with molecular weights of $2.3 \times 10^5$ and $3.0 \times 10^5$, respectively.

Blending of 90/10, 80/20, 70/30 and 50/50 (wt% ratio) of *i*-PP/EH32 and *i*-PP/EH57 was undertaken by heating and magnetically stirring *i*-PP and EH (32 or 57) copolymer with xylene for 2 h at 120°C in a reflux distillation apparatus. About 1% of 2-6-di-*tert*-butyl-4-methyl phenol was added to the solution as a stabilizer. The blend was cooled, precipitated with methanol kept standing for about 4 h and filtered, followed by air and vacuum drying at ambient temperatures, each for two days. *i*-PP was also treated in the same way as the blends for comparative study. Slab test specimen (50 mm × 50 mm × 0.6–0.7 mm) was prepared using a hot press machine which was set at 200°C for 8 min. The slabs were annealed at 100°C for 5 h and cut to the desired test specimen size.

### 2.2. Mechanical measurements

Dumbbell test specimens were prepared by die cutting of the slab samples. Tensile properties of the specimens were determined using a Shimazu Tensile Tester model AGS-G. The equipment was set at a constant cross-head speed of 10 and 5 mm/min for *i*-PP and *i*-PP/EH57, and *i*-PP/EH32, respectively. The size of the samples was 30 mm($L$) × 5 mm($W$) × 06–0.7 mm($T$) and the gauge length was 10 mm.

### 2.3. Wide-angle X-ray diffraction

WAXD measurement was carried out using a rotating-anode Rigaku X-ray generator (RU-300) operated at 40 kV and 240 mA. CuKα X-ray beams, which were monochromatized with a graphite monochromator, were directed onto the specimen through a pinhole collimator of 0.5 mm in diameter. As an X-ray detector, the IP system (MAC Science, DIP 220) was used. The distance of the specimen to the imaging plate was 84 mm.

In the drawing device [16], the samples were horizontally clipped to the sample holder and uniaxially drawn from both sides to remain the same illumination position at drawing rate 10 and 4 mm/min for *i*-PP and *i*-PP/EH57, and *i*-PP/EH32, respectively. After stretching the test specimen to the desired elongation (based on their stress–strain curves), drawing was halted and WAXD measurement was undertaken. The procedure was repeated until the sample was about to be cut or cut off during the drawing. The draw ratio (DR) was defined as follows: When the sample was cut off during drawing, the drawn specimen was taken out of the drawing device and the final DR was estimated from the elongated graduation marks in the specimen area which were illuminated with the X-ray beams. From this estimate and the drawing time, the DR was calculated by proportional allotment.

### 2.3. Atomic force microscopy

Atomic force microscopy (AFM) was performed in a dynamic mode using a Shimazu AFM Model SPM-9500J2. The scanner was placed on an air-spring vibration insulator and was stabilized for 1 h scanning to reduce the specimen drift, which was induced thermally. Silicon cantilever nanosensor type NCHR-16 with spring constant 42 N/m and resonance frequency 330 kHz was used to measure the vertical oscillation amplitude. The samples were broken under liquid nitrogen to maintain the globular domains of the EH copolymers.

### 2.4. Transmission electron microscopy

The morphologies of the undrawn and drawn blends of 70/30 *i*-PP/EH32 and 70/30 *i*-PP/EH57 were examined using JEOL TEM model JEM-100. The blends were, respectively, drawn to DR 6.2 and 7.4 at drawing rates of 4 and 10 mm/min during WAXD measurements. The samples were sliced into ultra-thin films and stained with ruthenium tetraoxide.

### 2.5. Small-angle X-ray scattering

SAXS measurement was carried out using SAXES Optics installed at BL-10C of the photon Factory, Tsukuba, Japan [17], where an incident X-ray from synchrotron radiation was monochromatized to the wavelength of the X-ray ($\lambda$) = 0.1488 nm with a double-crystal monochromator and focused to the focal point with a bent focusing mirror. The scattered X-ray was detected by one-dimensional position sensitive proportional counter of an effective length of 160 mm positioned at the distance of about 1.0 m from the sample holder. The camera distance was calibrated using the diffraction peaks of the collagen fiber (the long period = 67 nm) at the sixth, ninth and eleventh orders. Data were collected on a CAMAC system.

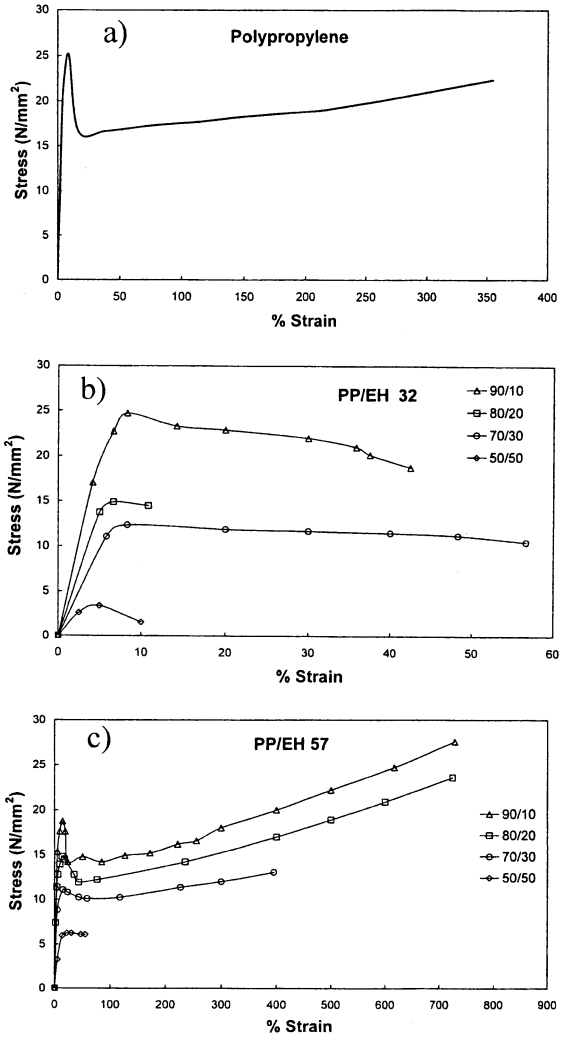


Fig. 1. Stress–strain curves of (a) pure *i*-PP film, (b) *i*-PP/EH32 film and (c) *i*-PP/EH57 film at room temperature.

## 3. Results and discussion

### 3.1. Mechanical properties

Fig. 1(a)–(c) shows the stress–strain curves of *i*-PP and the two blends (*i*-PP/EH 32 and *i*-PP/EH57). Pure *i*-PP exhibited a large, sharp stress drop by necking after the yield point. The *i*-PP/EH32 and *i*-PP/EH57 produced different stress–strain curves as shown in Fig. 1(b) and (c), respectively. It was found that the elongation of *i*-PP/EH32 was very small as compared with *i*-PP/EH57 and pure *i*-PP. Hence, the cross-head speed of the tensile tester was varied, viz. 4 mm/min for *i*-PP/EH32 to avoid the early cutting of the film and 10 mm/min for *i*-PP/EH57. These cross-head speeds (4 and 10 mm/min) were presumed to have only a slight effect on the tensile properties and had no effect on the morphological change since both speeds are very slow in polymer. The yield stress of 90/10 *i*-PP/EH32 was 24.72 $N/mm^2$ which gradually decreased to 3.39 $N/mm^2$ with the addition of 50% EH32 and its modulus also gradually decreased with the increase of EH32. The stress drop after the yield point of 90/10 *i*-PP/EH32 was small and disappeared with increase of EH32. In this report, 70/30 *i*-PP/EH32 showed the highest ultimate strain value in tensile mode followed by 90/10, 80/20 and 50/50 *i*-PP/EH32. On the other hand, the stresses at break point of *i*-PP/EH57 were remarkably higher than those of *i*-PP/EH32. It was also noted that the stress drops after the yield point appeared clearly, but the drop became less sharp than that observed in the pure *i*-PP with the addition of 10–20% EH57. Furthermore, the strain values at break point of 10–20% EH57 blend were significantly higher than those of *i*-PP/EH32.

## 4. Structural changes by WAXD measurements on drawing

### 4.1. Isotactic polypropylene

The WAXD patterns of the *i*-PP film exhibited four sharp crystalline ring reflections at 110, 040, 130 and 111 + [13$\bar{1}$ + 041] (monoclinic form; $a = 0.665$ nm, $b = 2.096$ nm, $c = 0.650$ nm, $\alpha = 90°$, $\beta = 90°20'$, $\gamma = 90°$), and a few weak crystalline reflections in the wide angle side as shown in Fig. 2. These results suggest its α-modification [18]. The *i*-PP film was represented by intense and moderate ring reflections demonstrating the unoriented crystalline and amorphous ring structures. When *i*-PP was drawn to DR 2.0–2.5 at drawing rates of 10 mm/min, two diffuse spots appeared clearly on the equator of the crystalline ring structure. These spots are assigned to 110 reflection, which are indicative of orientation of PP chains. At the same time, the diffuse spots between 110 and 130 reflections on the equator began to appear faintly. These are due to the oriented amorphous region and the paracrystalline smectic

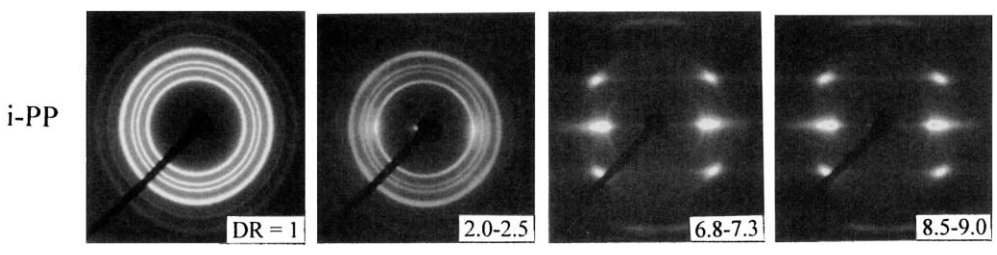


Fig. 2. WAXD patterns of pure *i*-PP film under drawing at room temperature.

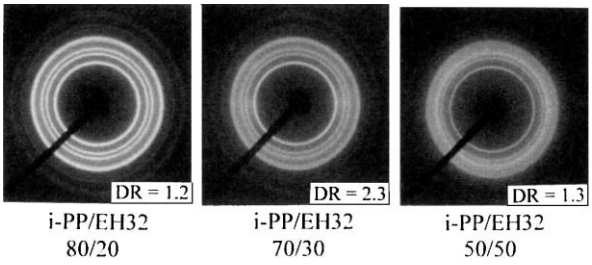


Fig. 3. WAXS patterns of 80/20, 70/30 and 50/50 *i*-PP/EH32 films before cutting by drawing at room temperature.

form [19,20]. The ring reflections were gradually transformed to equatorial spot reflections as seen at DR 6.8–7.3 in Fig. 2. These reflections representing the 110, 040, and 130 are broad due to their overlapping and the lattice disorder by shifting of molecular chains to the drawing direction. At DR 8.5–9.0, the spot reflections were intensified, while the ring reflections disappeared and only small arc reflections around the spots remained. These are due to some unchanged crystallites, the distorted orientation of polymer chains to the drawing direction and the division of the original crystallites to small ones by drawing. The structural changes of *i*-PP during uniaxial drawing are presented here in order to provide a better understanding on the results on structure of *i*-PP/EH32 and *i*-PP/EH57 treated in the following sections.

### 4.2. Immiscible blends

The blends of *i*-PP/EH32 copolymer were drawn at a low speed, viz. 4 mm/min in order to obtain maximal elongation taking account of their brittleness. Increase in the EH32 content from 10 to 50% led to the weakening of the crystalline ring reflections of the undrawn *i*-PP and this was simply due to the increase of the amorphous EH32. The WAXD patterns of 80/20, 70/30 and 50/50 *i*-PP/EH32 are shown in Fig. 3. The drawing of these blends was up to just before cutting. There were no significant changes on orientation observed during drawing except the 90/10 *i*-PP/EH32. The 70/30 *i*-PP/EH32 was cut at the onset of necking by drawing. On 50/50 *i*-PP/EH32, 040 reflection is much weaker than those of 80/20 and 70/30 blend ratio. This shows that the *b*-axis moved to the perpendicular direction for film surface.

The WAXD patterns of 90/10 *i*-PP/EH32 are shown in Fig. 4. The crystalline ring reflections of the undrawn *i*-PP/EH32 sample are due to the crystalline structure of *i*-PP. It was difficult to distinguish the amorphous EH32 copolymer from the amorphous structure of *i*-PP. At DR 2.7–3.0, two diffuse spots (110 reflection) on the equator and four reflection spots which were piled 111 reflections over $13\bar{1}$ + 041 reflections on the first layer, were clearly observed on the crystalline ring reflection of *i*-PP, indicating the presence of unoriented and oriented crystalline structures. When the blend was drawn to DR 4–4.3, the crystalline ring reflection became weak and the intensity of the six spots increased, which indicate the presence of oriented crystals. The onset of orientation of *i*-PP (DR 1.6) was delayed by the addition of EH32, even by 10% EH blending.

### 4.3. Miscible blends

The blends of *i*-PP/EH57 copolymer were drawn at a higher speed, viz. 10 mm/min, than that of the immiscible blends. This higher speed was possible due to their high elongations. The changes of WAXD patterns of 80/20 and 70/30 *i*-PP/EH57 under drawing are presented in Fig. 5. In drawing of 90/10 *i*-PP/EH57, the appearance and the change of crystalline reflection were almost the same as in *i*-PP except that the onset of orientation is late.

The undrawn 80/20 *i*-PP/EH57 exhibited a slight increase of broad amorphous ring reflection as compared with *i*-PP and 90/10 *i*-PP/EH57 due to the increase of EH57 copolymer. The orientation of 80/20 *i*-PP/EH57 was clearly observed at DR 2.2 as shown by the appearance of poor equatorial spots on the crystalline ring reflections in Fig. 5 (upper). Drawing to DR 3.6–4.1 resulted in the appearance of six spots on the equator and four spots on the first layer on the crystalline ring reflections. These results indicate the coexistence of an oriented and an unoriented crystalline structure. In further drawing to DR 7.5–8.0, the intensity of the ring reflections weakened while the six spots sharpened due to the orientation of the crystalline structure to result in a more ordered form. This observation is in contrast with the result on the drawing of the immiscible blend where orientation was not observed when more than 20% EH32 was added.

Fig. 5 shows (lower) that WAXD patterns on the elongation of 70/30 *i*-PP/EH57 were the same as those of 80/20 *i*-PP/EH57 except for the even slower transformation rate of the ring reflections to the spot reflections. The onset of

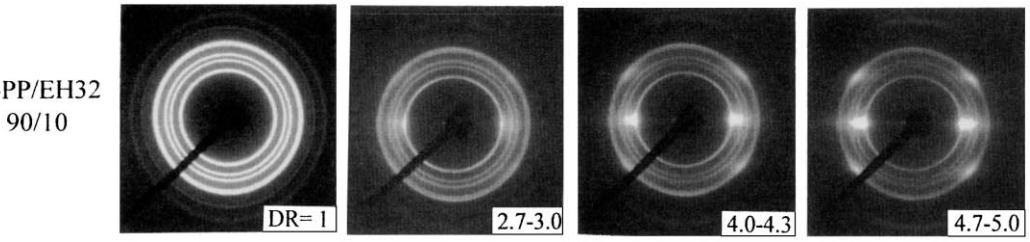


Fig. 4. WAXD patterns of 90/10 *i*-PP/EH32 film under drawing at room temperature.

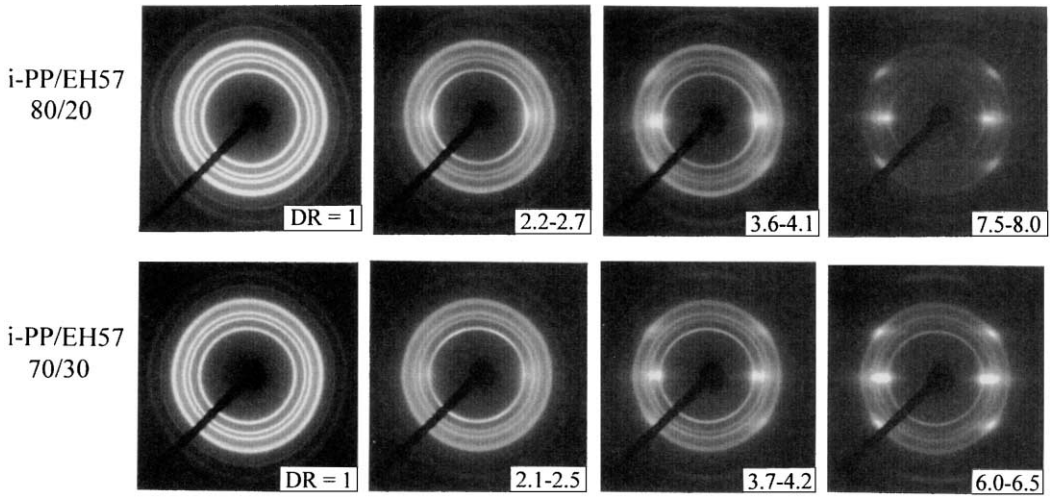


Fig. 5. WAXD patterns of 80/20 and 70/30 *i*-PP/EH57 films under drawing at room temperature.

orientation occurred when the film was drawn to DR 1.65, and this was the fastest occurrence among the blends. By further drawing, the transformation to the spot reflections gradually proceeded. It is assumed that the molecular chains of EH57 copolymer in amorphous state existed between lamellae of *i*-PP [21] and that the transformation of *i*-PP from the lamellae structure to the extended structure easily proceeded. At DR 6.0–6.5, the crystalline ring reflections of 70/30 *i*-PP/EH57 remained clearer than that of the 80/20 *i*-PP/EH57. Fig. 6 shows equatorial intensity profiles of WAXD patterns of 70/30 *i*-PP/EH57 in Fig. 5 and each profile was divided in each crystalline reflection and amorphous phase. The sharp crystalline reflections (as seen in Fig. 6(a)) are broken by drawing and transformed to one broad reflection by overlapping of the broadened crystalline reflections (Fig. 6(d)). It is also noted that the amorphous phase content reached the maximum at (b) DR 2.1–2.5

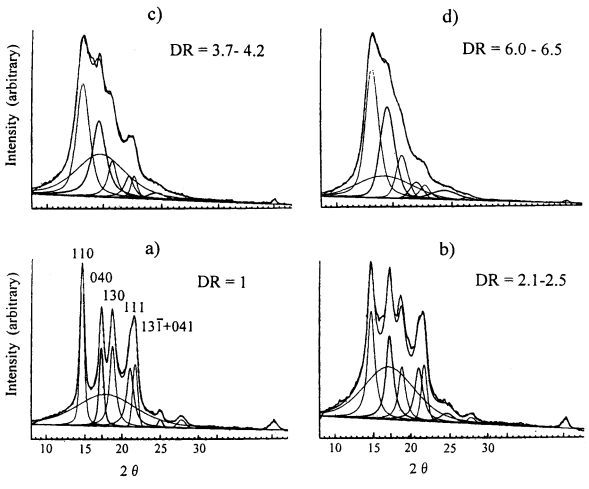


Fig. 6. Intensity profiles on the equator of WAXD patterns of 70/30 *i*-PP/EH57 film. Each profile was divided on each crystalline reflection and amorphous phase.

under drawing and then decreased gradually as drawing. This is due to the orientation in amorphous phase and the smectic form has appeared as seen in the drawing of pure *i*-PP, and furthermore, a part of the broken crystal might have transformed to the amorphous phase. The integral breadth of 110, 040 and 130 crystalline reflections of 70/30 *i*-PP/EH57 was shown in Fig. 7. The integral breadth of 110 and 040 reflections increased suddenly at DR 1.65 and propagated flatly up to DR 3. This increase is due to disordering of the crystal lattice by necking at DR 1.65, which suggests that the lamellae crystals were broken by drawing and changed to smaller crystallites. Further increase in integral breadth of these reflections and 130 crystalline reflection occurred from DR 3. This shows that the crystallites divided further into smaller ones by drawing and disordered by shifting of molecular chains parallel to drawing direction.

In the case of 50/50 *i*-PP/EH57, the WAXD pattern exhibited an increase of the amorphous structure, while the 040, 130 crystalline ring reflections were broader than the reflections of the blends containing 20 and 30% EH57. At drawing to above DR 2.3, this blend film became thin and was cut by necking. It is not suitable for drawing the blend of above 50% EH57 content.

### *4.4. Morphologies as revealed by AFM and TEM*

The difference of mechanical properties of 70/30 *i*-PP/EH32 and 70/30 *i*-PP/EH57 is discussed from viewpoints of morphology. For the miscible blends of *i*-PP/EH57, undrawn and drawn samples did not show much change in morphology and this result is in accordance with the Yamaguchi's results of homogeneous structure [12]. In the immiscible blends, the results were different; undrawn and drawn samples of 70/30 *i*-PP/EH32 were broken under liquid nitrogen and the surfaces were observed by AFM as shown in Fig. 8. In the undrawn sample, the globular domain structure of the diameter of which is 1–3 μm is

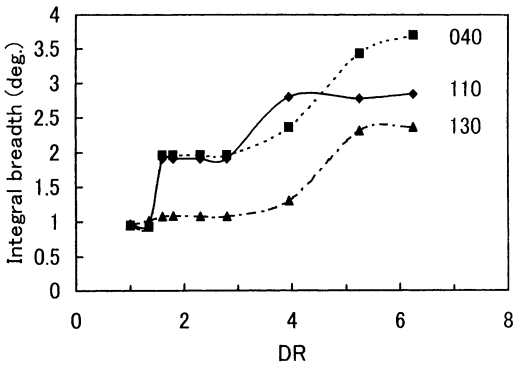


Fig. 7. Changes in the integral breadth of 110, 040 and 130 reflections of 70/30 *i*-PP/EH57 film. No correction was done for the instrumental broadening.

observed as seen in Fig. 8(a). To further elucidate the inside structure of the globular domains, TEM was taken on the sample cut by diamond knife and stained by ruthenium tetraoxide. It was found that the black stained globular parts were EH copolymer. The dimension of these globular parts was in accordance with that by AFM as seen in Fig. 9.

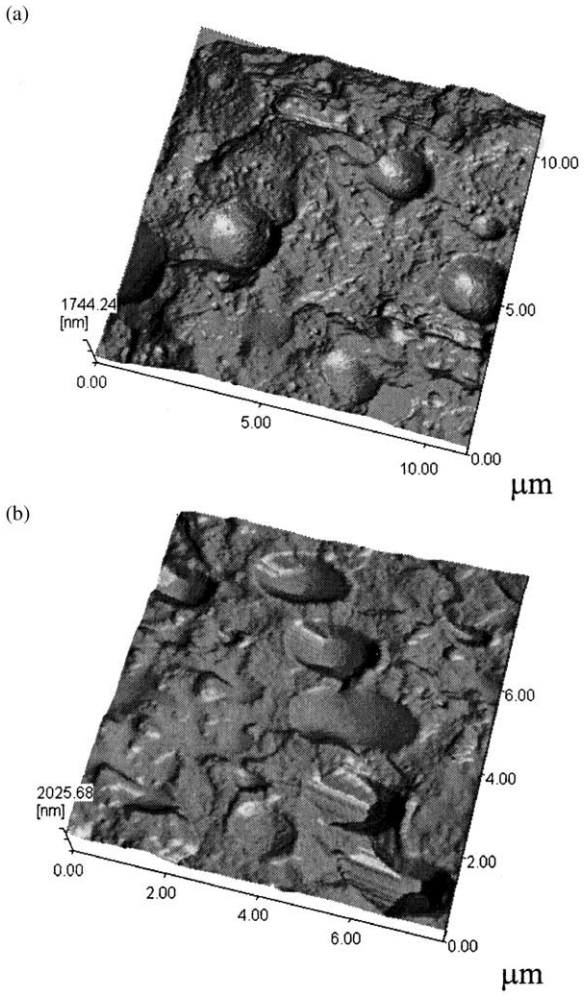


Fig. 8. AFM of (a) undrawn and (b) drawn (DR 2) 70/30 *i*-PP/EH32 film.

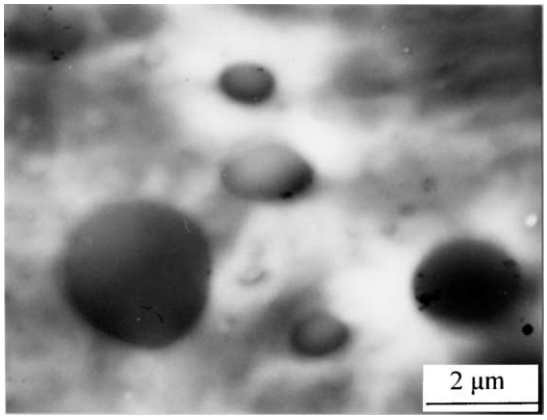


Fig. 9. TEM of undrawn *i*-PP/EH32 film.

The blend of *i*-PP/EH32 is a two-phase system, i.e. the EH32 copolymer is represented by black globular structure and *i*-PP forms the white matrix. When this blend was drawn, the globular domains changed to an ellipse, the long axis of which is parallel to stretching direction as seen in Fig. 8(b). The deformation of globular domains was about double in all observations. At above DR 2, *i*-PP/EH32 was broken from the interface with the domains because the stress was concentrated on the interface. On the other hand, *i*-PP/EH57 has no domain structure because molecular chains of EH copolymers are incorporated within

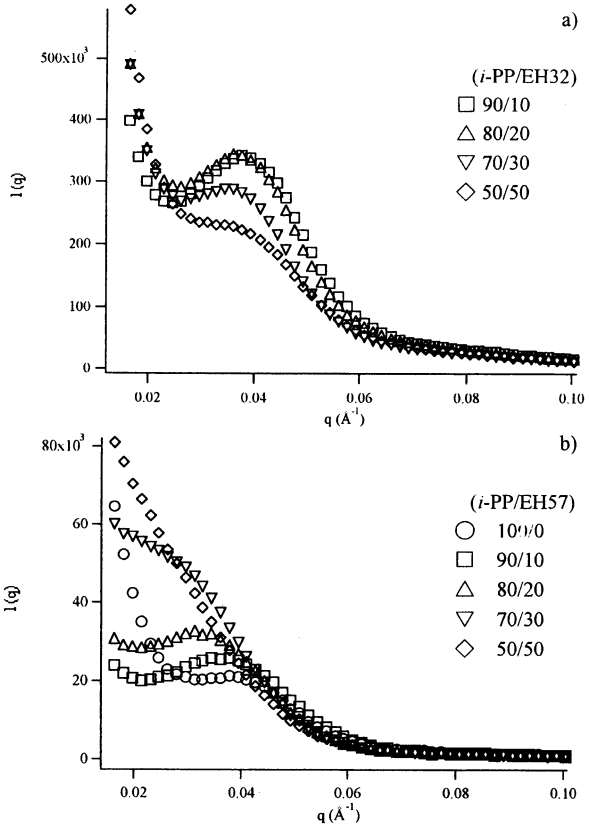


Fig. 10. SAXS intensity profiles of (a) *i*-PP/EH32 and (b) *i*-PP/EH57 film.

amorphous parts of *i*-PP. Therefore, a stretching force propagates smoothly to all parts in the sample. It is understood from these structural viewpoints that the stress and strain at breaking point of 70/30 *i*-PP/EH57 were higher than that of 70/30 *i*-PP/EH32.

### 4.5. Small-angle X-ray scattering

Fig. 10 shows SAXS intensity profiles of (a) *i*-PP/EH32 and (b) *i*-PP/EH57 with four blend ratios. Here, the intensity of pure *i*-PP (100/0 *i*-PP/EH57) shown in (b) was weakened to the half value by inserting the aluminum plate. In the immiscible blends of *i*-PP/EH32 in Fig. 10(a), the scattering peak intensity decreased in proportion to the increase in EH copolymer content, but its position did not change by the ratio. This peak position shows the long period (16.5 nm) of *i*-PP, which corresponds to the repeat distance of lamellae of *i*-PP and no influence of EH copolymer was observed. On the other hand, in the miscible blends of *i*-PP/EH57 in Fig. 10(b), the position (q) of the scattering peak decreased by the increase in EH57 copolymer content. This is due to the increase of amorphous parts between lamellae, that is, the long period increased, e.g. 100% *i*-PP = 16.5 nm, 90/10 *i*-PP/EH57 = 17.4 nm, 80/20 = 19.0 nm, 70/30 = 20.3 nm, and 50/50 *i*-PP/EH57 has no obvious peak. The *i*-PP/EH57 exhibited that the molecular chains of EH57 copolymer joined the amorphous parts between lamellae of *i*-PP, and this resulted in the increase in the distance between lamellae. This increase of amorphous parts contributed to the sustained presence of the crystallite under higher DR. Consequently, the films from the miscible blend are expected to be drawable and more of higher impact resistance. When these miscible blends were stretched, it is assumed that the molecular chains of oriented crystallites can move easily to the stretching direction due to the presence of amorphous parts between lamellae.

## 6. Conclusions

The blends of *i*-PP and EH copolymer were studied to improve the mechanical properties of *i*-PP. For this purpose, we examined the structural changes of *i*-PP/EH32 and *i*-PP/EH57 films under uniaxial drawing using in situ WAXD equipment. The relationship between this structural change and mechanical properties was discussed. The *i*-PP/EH32 samples formed two-phase structure and are not drawable up to higher DR because they are broken from the interface of domain by drawing at room temperature except 90/10 *i*-PP/EH32. On the other hand, in 80/20 and 70/30 *i*-PP/EH57, the molecular chains of EH57 copolymer are incorporated into amorphous phase between lamellae of *i*-PP and these blends could smoothly be elongated up to higher DR. It was also noted that the transformation of these blends from crystalline ring reflections to the crystalline spot reflections propagated gradually from a small strain up to larger DR. Further, these blends demonstrated the coexistence of the unoriented and oriented structure up to large DR. From the structural views of this study, it is expected that the 80/20 and 70/30 *i*-PP/EH57 films have been much improved in brittleness compared with the pure *i*-PP film.

## Acknowledgements

The authors gladly acknowledge the scholarship to E.L.B. under JSPS-DOST RONPAKU Program. Thanks are also due to TOSOH Corp., Japan and JGS Petrochemical Corp., Phils. for giving us the raw materials, Dr Yamaguchi and Elsie David for their discussions, and Mr M. Ohara for conducting TEM.

## References

[1] Martuscelli E, Silvestre C, Abate G. Polymer 1982;23:229.
[2] Bedia EL, Astrini N, Sudarisman A, Sumera F, Kashiro Y. J Appl Polym Sci 2000;78:1200.
[3] Danesi S, Forter R. Polymer 1978;19:448.
[4] Ishikawa M, Sugimoto M, Inoune T. J Appl Polym Sci 1996;62:1495.
[5] Ha CS. J Appl Polym Sci 1986;32:6281.
[6] Gupta AK, Purwar SN. J Appl Polym Sci 1984;29:1079.
[7] Gupta AK, Purwar SN. J Appl Polym Sci 1984;29:1595.
[8] Gupta AK, Purwar SN. J Appl Polym Sci 1984;29:3513.
[9] Gupta AK, Purwar SN. J Appl Polym Sci 1986;31:535.
[10] Gupta AK, Purwar SN. J Appl Polym Sci 1991;42:297.
[11] Nitta K, Okamoto K, Yamaguchi M. Polymer 1998;39:53.
[12] Yamaguchi M, Miyata H, Nitta K. J Appl Polym Sci 1996;62:87.
[13] Yamaguchi M, Nitta K, Miyata H, Masuda T. J Appl Polym Sci 1997;63:467.
[14] Yamaguchi M, Miyata H, Nitta K. J Polym Sci, Polym Phys 1997;35:953.
[15] Yamaguchi M, Suzuki K, Miyata H. J Polym Sci, Polym Phys 1999;37:701.
[16] Murakami S. Nippon Kagaku Kaishi 2000(2000):141.
[17] Ueki T, Hiragi Y, Izumi Y, Tagawa H, Kataoka M, Muroga M, Matsushita T, Amemiya Y. Photon Factory Rep IV 1983:70.
[18] Addink EJ, Beintema J. Polymer 1961;2:185.
[19] Nadella HP, Henson HM, Spruiell JE, White JL. J Appl Polym Sci 1977;21:3003.
[20] Nadella HP, Henson HM, Spruiell JE, White JL. J Appl Polym Sci 1978;22:3121.
[21] Yamaguchi M. Dissertation (structure and mechanical properties for binary blends of polypropylene with ethylene–α-olefin copolymer). Japan: Kyoto University, 1999. p. 33.